Tailoring the Formation and Stability of Self-Assembled Structures from Precisely Engineered Intrinsically Disordered Protein Polymers: A Comprehensive Review

Fathima T. Doole[a], Christopher P. Camp[b] and Minkyu Kim[b,c,d†]

[a]*Department of Chemistry and Biochemistry, University of Arizona, Tucson, AZ 85721, USA*

[b]*Department of Biomedical Engineering, University of Arizona, Tucson, AZ 85721, USA*

[c]*Department of Materials Science and Engineering, University of Arizona, Tucson, AZ 85721, USA*

[d]*BIO5 Institute, University of Arizona, Tucson, AZ 85721, USA*

Keywords

Intrinsically Disordered Protein, protein polymer, self-assembly, stimulus responsiveness, structural stability

Abstract

Intrinsically disordered proteins (IDPs) are a class of proteins that lack stable three-dimensional structures. Despite their natural tendency to be disordered, precise modulations of molecular parameters (e.g., sequence, length) through biomolecular engineering tools and control of environmental conditions tailor the formation of dynamic self-assembled structures. In addition to designing structures that respond to external stimuli for specific biotechnological applications (e.g., biosensors), other applications require stable structures (e.g., engineered tissues, drug delivery vehicles) that resist unintended changes and disassembly across various environmental conditions, such as different concentrations and temperatures. This review provides a comprehensive understanding of the design and engineering principles that govern the self-assembly of biosynthetic IDPs and their stability. Specifically, elastin-like polypeptides (ELPs) are highlighted as a prominent example of biosynthetically designed, thermoresponsive IDPs. Examples include ELPs that form various self-assembled structures by themselves as ELP homopolymers or diblock copolymers, ELPs combined with other IDPs in diblock copolymers, and ELP-based polymer hybrids containing functional (bio)molecules. It is anticipated that the efforts to enhance the stability of self-assembled structures through the precise engineering of IDP-based polymers have expanded the potential for diverse biotechnological applications in tissue engineering, drug delivery, diagnostic assays, and biomedicine.

1. Introduction

Intrinsically disordered proteins (IDPs) comprise all natural and synthetic proteins that lack stable three-dimensional secondary, tertiary or quaternary structures [1]. It is reported that roughly 10% of all natural proteins are intrinsically disordered [2]. The physicochemical properties of IDPs are derived from their properties and arrangement of constituent amino acids, and their sequence complexity tends to be low [1]. Examples of natural IDPs include the Non-A beta component of the Alzheimer's disease amyloid precursor, $p21^{Waf1/Cip1/Sdi1}$, anti-Σ-28 factor, calpastatin, microtubule-associated protein tau, and the transactivation domain of transcription factors [2].

The self-assembly of natural IDPs from nanostructures to larger structures is uncommon, but biosynthetically designed IDP homopolymers, IDP-based block copolymers, and IDP-based polymer hybrids containing functional (bio)molecules form a variety of self-assembled structures, such as micelles, nanofibers, and vesicles (Fig. 1). The self-assembly is controlled by diverse design parameters such as sequence, length, charge, hydrophobicity of IDPs and environmental conditions like concentration, temperature, and pH. Biomolecular engineering tools enable the precise modulation of sequences and chain lengths, as well as provide opportunities to engineer IDPs at the amino acid level to correlate diverse self-assembled structures with those parameters and environmental conditions. Among various biosynthetic IDPs, elastin-like polypeptides (ELPs) have been extensively investigated.

ELPs have initially gained attention due to their thermoresponsive behaviors that facilitate non-conventional protein purification methods [3]. ELP or ELP-containing proteins and peptides can be purified without conventional chromatography. Briefly, the solution is heated to separate the ELP into a coacervate phase such that the ELP is captured by centrifugation. Then, the ELP pellet is dissolved in cold solution and centrifuged to capture impurities that do not dissolve. This process is repeated several times to yield highly pure ELP. Furthermore, this purification method can be utilized to obtain target proteins and peptides by genetically fusing self-cleaving sequences, such as intein, between the ELP and target sequences [4] to avoid expensive proteolytic tag removal or chromatography techniques.

After characterizing and implementing the intrinsic stimulus-responsive behaviors of ELP-based polymers and polymer hybrids, the discovery of diverse self-assembled ELP-based structures opened a new area of focus. Together with the overall biocompatibility of ELPs, including non- or low-immunogenic profiles [5-8], the self-assembled structures from ELP-based

polymers have been applied to a broad range of biomedical applications, such as drug delivery [9-11], vaccine carriers [12], tissue engineering [13, 14], and antimicrobial therapies [15-18]. Diverse ELP-based polymers, including the synthesis and use of ELP-based materials and self-assembled structures for potential biomedical applications, are well-covered in multiple review articles [6, 19-23].

While dynamic self-assembly that changes depending on environmental conditions are useful for biomedical applications such as drug delivery [9-11], self-assembled structures that are stable across various environmental conditions are also required in other biomedical applications, including the use of such materials as artificial extracellular matrices in tissue engineering [24]. To form stable structures through a range of external environments, biosynthetic IDP polymers must be engineered with an understanding of the design parameters that are responsible for the formation of self-assembled structures as well as modifications that can be made for enhanced structural stability.

In this review, tailoring the formation of various self-assembled IDP polymer-based structures and methods to improve their stability are discussed (Fig. 1) with particular focus on ELP-based polymers due to their unique physicochemical properties, stimulus-responsive behaviors, and high level of customizability, all of which are important properties for a variety of biotechnological applications. Beyond the sequence information and the self-assembly behaviors of ELP homopolymers, the self-assembly characteristics of ELP-based block copolymers, composed of only ELP blocks or ELP blocks with other biosynthetic IDP blocks, such as resilin-like polypeptide (RLP) and silk-like polypeptide (SLP), are described (Fig. 1b). As a reference for readers when engineering specific self-assembled structures using IDP-based polymers (Fig. 1c), the guidelines of protein polymer sequences, molecular design parameters, and environmental conditions are summarized in Table 1. Moreover, structures formed by ELP-based polymer hybrids containing functional (bio)molecules, such as self-assembling DNA, are highlighted. Finally, the progress to stabilize the IDP-based self-assembled structures (Fig. 1d) is discussed to provide the reader with an understanding of the diverse methods available to utilize unique self-assembled nanostructures and larger -structures for their desired applications.

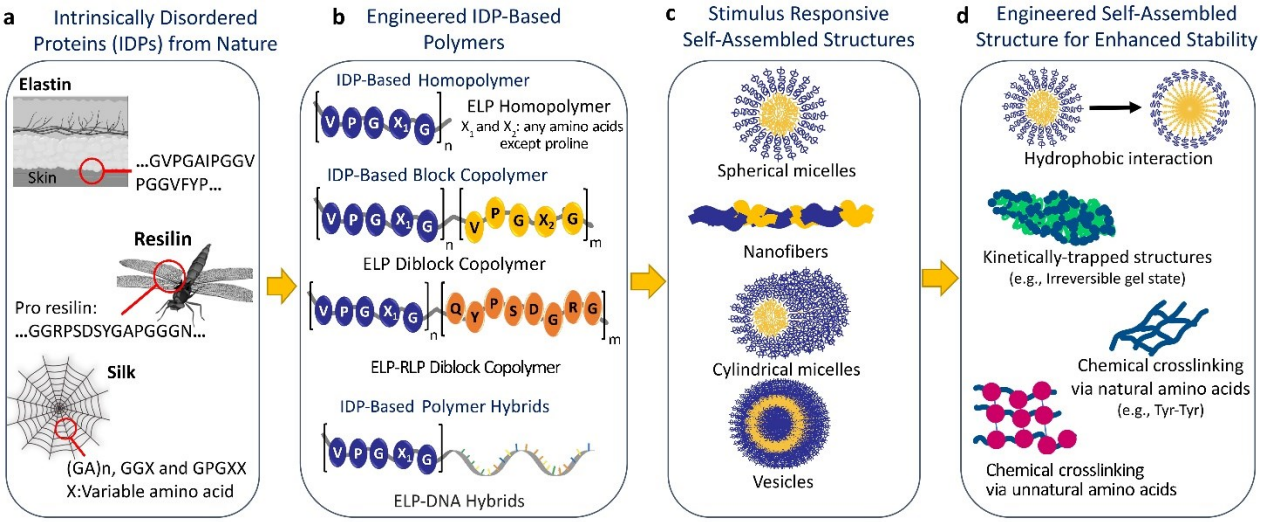

Fig. 1. Formation and stability of self-assembled structures from engineered intrinsically disordered protein (IDP) polymers. Repeated consensus sequences of engineered IDPs, extracted from natural IDPs, can be used to prepare various IDP polymers, including IDP homopolymers (e.g., elastin-like polypeptide (ELP) homopolymer), block copolymers with distinct blocks from the same type of IDP (e.g., ELP) or blocks of different IDPs (e.g., ELP with silk-like polypeptide, SELP, or resilin-like polypeptide, ELP-RLP), and IDP fusions with other (bio)molecules (e.g., ELP-DNA). Thermoresponsive IDP homopolymers, such as ELP, or IDP block in block copolymers, can self-assemble into diverse structures that are controlled by modulating molecular design parameters (e.g., sequences, physicochemical properties) and environmental conditions (e.g., solution temperatures, pH, and salt concentrations). Engineering IDP sequences (e.g., unnatural amino acids) or blocks can further enhance the stability of self-assembled structures.

Table 1. Summary of biosynthetic IDP sequences, molecular design parameters, and environmental conditions to prepare various dynamic self-assembled structures.

IDP-Based Polymer Design	Molecular Parameters	Environmental Conditions		Self-Assembled Structures	Reference
		Temperature	Concentration		
ELP Homopolymer					
$(VPGLG)_n$	n=20	5 - 50 °C	0.05 mg/mL	Particle ([1]d = 400 nm at 5°C – d = 760 nm at 50 °C)	45
		5 - 50 °C	0.1 mg/mL	Particle (d = 400 nm at 5°C – d = 760 nm at 30 °C)	
		5 - 50 °C	0.5 mg/mL	Particle (d = 2 µm)	
		5 - 50 °C	1 mg/mL	Particle (d = 1.5 µm)	
	n=40	5 - 50 °C	0.05 mg/mL	Particle (d = ~1 nm at 5°C – d = ~375 nm at 50 °C)	
		5 - 50 °C	0.1 mg/mL	Particle (d = ~1 nm at 5°C – d = ~500 nm at 50 °C)	
		5 - 50 °C	0.5 mg/mL	Particle (d = ~200 nm at 5°C – d = ~770 nm at 50 °C)	
		5 - 50 °C	1 mg/mL	Particle (d = ~200 nm at 5°C – d = ~750 nm at 50 °C)	
	n=80	5 - 50 °C	0.05 mg/mL	Particle (d = ~1 nm at 5°C – d = ~420 nm at 50 °C)	
		5 - 50 °C	0.1 mg/mL	Particle (d = ~1 nm at 5°C – d = ~500 nm at 50 °C)	
		5 - 50 °C	0.5 mg/mL	Particle (d = ~1 nm at 5°C – d = ~700 nm at 50 °C)	
		5 - 50 °C	1 mg/mL	Particle (d = ~1 nm at 5°C – d = ~500 nm at 50 °C)	
	n=160	5 - 50 °C	0.05 mg/mL	Particle (d = ~1 nm at 5°C – d = ~330 nm at 50 °C)	
		5 - 50 °C	0.1 mg/mL	Particle (d = ~1 nm at 5°C – d = ~300 nm at 50 °C)	
		5 - 50 °C	0.5 mg/mL	Particle (d = ~1 nm at 5°C – d=~650 nm at 50 °C)	

		5 - 50 °C	1 mg/mL	Particle (d = ~1 nm at 5°C – d = ~660 nm at 50 °C)	
$(VGGVG)_n$	n=5	Undefined	Undefined	Nanofibers	50
$(LGGVG)_n$	n=7	Room temperature	20 mg/mL	Fiber Bundles (d = 4.5 nm to 48 nm with length of 1.15 µm)	51
ELP Diblock Copolymer					
$[(VPGEG)_1\text{-}(IPGAG)_4]_m$ - $[(VPGFG)_1\text{-}(IPGVG)_4]_n$	m=14, n=16	25 °C	20 mM NaOH	Spherical Micelles (d = 47nm)	55
		25 °C	Phoshphate buffer (pH 7.4)	Spherical Micelles (d = 57nm)	
		25 °C	Water	Spherical Micelles (d = 54 nm); Cylindrical Micelles (d = 50 nm)	
$[(VPGVG)_2\text{-}VPGEG\text{-}(VPGVG)_2]_m$ - $(VGIPG)_n$	m=10, n=60	-	1-8 mg/mL	Spherical Micelles	56
			<50 mg/mL	Cylindrical Micelles	
			50-100 mg/mL	Fibrillar Network	
			>100 mg/mL	Lyotropic Hydrogel	
$[(VPGVG)_1(VPGAG)_8(VPGGG)_7]_m\text{-}[(VPGVG)_5]_n$	m:n = 1:2 ~ 2:1	40 °C		Spherical Micelles	57
$G[(VPGIG)_m\text{-}(VPGSG)_n]Y$	m=18, n=18	>32 °C	25 µM	Nanostructures (d = >200nm)	58
	m=24, n=24	>24 °C	25 µM	Nanostructures (d = >200nm)	
	m=36, n=36	>22 °C	25 µM	Nanostructures (d = ~200nm)	
	m=48, n=48	24 - 60 °C	26 µM	Nanoparticles (d = ~40 nm at ^{2}CMT = 25 °C)	
	m=96, n=96	16 - 60 °C	27.5 µM	Nanoparticles (d= ~80 nm at CMT = 20 °C)	
$G[(VPGIG)_m(VPGAG)_n]Y$	m=48, n=48	24 - 48 °C	25 µM	Nanoparticles (d = ~40 nm at CMT = 25 °C)	
	m=96, n=96	16 - 46 °C	25 µM	Nanoparticles (d = ~80 nm at CMT = 20 °C)	
SLP-ELP Block Copolymer					
$(GAGAGS)_n\text{-}(GVGVP)_4(GYGVP)(GVGVP)_3$	n=1	>20 °C	-	Micelles (d = 120 nm)	77

	n=2	>20 °C	-	Micelles (d = 110 nm)	
	n=4	>20 °C	-	Micelles (d = 140 nm)	
RLP-ELP Block Copolymer					
$(QYPSDGRG)_m$-$[SGVPG]_n$ or $(QYPSDGRG)_m$-$[VGVPG]_n$	See details in Table 2			Spherical Micelles or Cylindrical Micelles	60
G-$(QYPSDGRG)_m$-$[(A/G)GVPG]_{80}$	m=40,60,80 where ϕ (RLP volume fraction) = 0.45-0.70	10 - 25 °C	30 wt%	Hexagonally Packed Cylinders	61
	m=100 where ϕ > 0.70	10-40 °C	30 wt%	Lamellae Structures	
	ϕ > 0.70	10 - 25 °C	50 wt%	Lamellae Structures	
$[GGRPSDSYGAPGGGNGGRPSSSYGAPGQGN]_n$-$[VPAAGVPAFGVPAAGVPAGGVPAAGVPAGF]_m$	n>=6, m = 6	<4 °C	-	Vesicles (d = 272-702 nm)	62
	n=24, m=12	>55 °C	-	Micelles (d = 68 nm)	
ELP-Based Hybrids					
[3]$ELP(VPGFG)_n$- [4]$CLP[(GPO)_4GFOGER(GPO)_4GG]$	n=6	4 °C - 65 °C	-	Nanoparticles (d = 50 ~250 nm; d=80–100 nm at room temperature and 150–250 at physiological temperature)	63
$ELP(VPGFG)_n$ – Oligonucleotides	n=6	20 °C - 60 °C	-	Spherical Micelles d=28 to 60 nm	64
$ELP(VPGAG)_n$ -C_{16}	n=3	-	ELP-C16 : Phospholipid = 4:1	Cylindrical Micelles (d =12.5 nm, length = 282 nm)	65
	n=3	-	ELP-C16 : Phospholipid = 1:1	Cylindrical Micelles (d=13.2 nm, length = 71 nm)	
$(VPGSG)_m$-$(IPGVG)_n$- antimicrobial peptide	m=50, n=60	-	-	Nanofibers	18

[1]d=diameter; [2]CMT=critical micelle temperature; [3]The transition temperature of ELP block needs to be lower than the melting temperature of CLP block; [4]CLP=collagen-like peptide

1.2. Natural Elastin-Inspired Monomers for Elastin-Like Polypeptides

Elastin is a natural intrinsically disordered protein and is one of the major extracellular matrix proteins (Fig. 1a). Elastin is responsible for controlling tissue elasticity and it is found in a variety of tissues including skin, lungs, blood vessels, and cartilage [25, 26]. Tropoelastin, the ~60 kDa precursor of elastin, comprises repetitive proline (P)-rich and glycine (G)-rich hydrophobic domains, as well as a large percentage of valine (V) and alanine (A) residues (Fig. 2). G and P residues in each hydrophobic domain are critical to maintain the primary IDP structure, with P disrupting the formation of specific 3D folded structures [27].

Elastin-like polypeptides (ELPs) are artificially engineered protein polymers derived from the repeating amino acid sequences in tropoelastin [3]. The P-rich hydrophobic domain from tropoelastin (Fig. 2) inspired the canonical ELP pentapeptide monomer sequence, $(VPGX_{aa}G)$, where X_{aa} is a guest residue that represents any amino acid except P [28]. The monomer sequences can be repeated, $(VPGX_{aa}G)_n$, and biosynthesized to produce ELPs. While V and G are typically observed in the first and third positions of the pentapeptide sequence, they can be replaced by isoleucine (I) and A, respectively [29, 30]. In addition to the representative ELP pentapeptide monomer sequence, there are other monomer sequences derived from different domains in tropoelastin, such as pentapeptide (e.g., KGGVG [31], VGGVG [32, 33], GVGVP [34]), heptapeptide (e.g., LGAGGAG [35]), and nonapeptide monomer sequences (e.g., LGAGGAGVL [35]), which have been biosynthesized to prepare physically and chemically diverse ELPs.

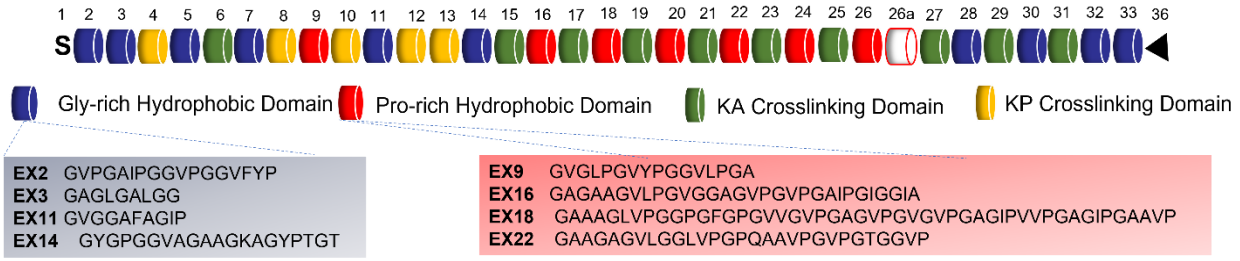

Fig. 2. Schematic representation of the human tropoelastin gene. The locations of G-rich hydrophobic (Blue) and P-rich hydrophobic (Red) domains are shown in addition to Lysine-Alanine (KA) and Lysine-Proline (KP) crosslinking domains (Green and Yellow) [36]. Natural exon sequences from G-rich and P-rich domains are demonstrated through randomly selected examples and are shown in the colored boxes. The letter S represents the initial signal peptide and

the triangle at the end represents the last peptide, which is hydrophilic. Complete sequences for all exons can be found at elsewhere [36].

2. Tailoring the Formation of Self-Assembled Structures from Engineered IDP-Based Polymers

2.1. Macromolecular Self-Assembly of ELP Homopolymers

A homopolymer is the simplest type of polymer, composed of a linear chain of identical monomers. ELP homopolymers, for example, are often comprised of the repeating ELP pentapeptide monomer, $VPGX_{aa}G$, and contain the same X_{aa} guest residue within every monomer (Fig. 1b). A primary characteristic of ELPs is their reversible phase transition at certain solution temperatures, defined as the lower critical solution temperature (LCST). ELPs exhibit extended random coils below the LCST because the hydrophobic side chains are hydrated by ordered water molecules, making the ELP soluble in aqueous buffers. When the solution temperature increases above the LCST, ELPs transform from random coils to β-spiral structures, consisting of consecutive type II β-turns. During this transformation, ELPs expel the bound water molecules, leading to the exposure of hydrophobic side chains. This triggers temperature-responsive, reversible phase separation or coacervation of ELPs, which form self-assembled structures for selected ELP homopolymers [37, 38].

The LCST of ELP is a function of its molecular design parameters and environmental conditions, such as the guest residues within the monomers, ELP molar mass, ELP concentrations, salt concentrations, salt types, and pH. In general, ELPs that contain more hydrophobic guest residues have a lower LCST compared to ELPs with more hydrophilic guest residues [37, 39, 40]. The molar mass of ELP is inversely correlated to the LCST where an increase in the ELP molar mass generally leads to a decrease in LCST [41]. In addition, the LCST can be reduced by increasing concentrations of ELP [41] and increasing concentrations of kosmotropic salts consisting of Cl^- or greater in the Hofmeister series [42]. Furthermore, the solution pH influences the ELP LCST when ionizable amino acids are present as guest residues [43, 44].

While most ELP homopolymers coacervate or phase-separate from aqueous solutions at temperatures above their LCST, selected ELPs can self-assemble into specific structures when the environmental conditions are controlled. Unsworth and coworkers studied the self-assembly of ELP homopolymers of $(VPG\underline{L}G)_n$, where the underlined sequence is the guest residue in each ELP

monomer, and n is 20, 40, 80, 160 [45]. The concentration of $(VPGLG)_{20}$ influenced the size of the self-assembled ELP particles that formed in aqueous solutions above the LCST. At concentrations less than 0.1 mg/mL, the particle was ~500 nm in diameter. However, upon cooling below its LCST, the ELP turned into micron-scale aggregates that were unstable in solution and did not resolubilize when the concentration was increased above 0.5 mg/mL [45]. In addition to investigating the effects of ELP concentrations on ELP structures above its LCST, it was identified that the ELP chain length is inversely correlated with the size of the temperature-triggered, self-assembled particles. Moreover, the zeta potential of self-assembled particles at 37 °C revealed that ELPs with relatively hydrophobic guest residues, such as $(VPGLG)_{40}$, exhibited negative zeta potential values of higher magnitude compared to ELPs with less hydrophobic, or relatively more hydrophilic, guest residues, such as $(VPGVG)_{40}$ [45]. However, self-assembled particles with less hydrophobic guest residues were unstable since the zeta potential values were between -30 mV and 30 mV, whereas particles tend to be more stable when the zeta potential is greater than 30 mV or less than -30 mV [46],[47]. No particular relationships were observed between the particle sizes and guest residues, and none of the tested ELP homopolymers constructed particles with diameters below 200 nm, which can be critical for applications such as drug delivery [48]. Therefore, a careful modulation of all aforementioned parameters is required to design and utilize self-assembled ELP structures for particular biomedical applications [49].

Distinct self-assembled structures have also been reported for other ELP homopolymers that deviate from the $VPGX_{aa}G$ sequence. Among those are ELPs composed of monomers with the sequence $X_{aa}GGZ_{aa}G$, which was derived from the G-rich hydrophobic domain of tropoelastin (Fig. 2). The X_{aa} and Z_{aa} positions are typically filled with some combination of V or L amino acids [32]. The comparison of self-assembled ELP structures from $(VGGVG)_n$ and $(LGGVG)_n$ identified that the additional $–CH_2$ in the side chain of L residues resulted in different morphologies [50]. When the solution temperature was increased above the LCST of each designed ELP, $(VGGVG)_n$ turned into well-defined, self-assembled fibers with bead-on-string morphologies after prolonged incubation above its LCST at ambient temperature (e.g., 25°C) [50]. On the other hand, $(LGGVG)_n$ transformed into fiber bundles with diameters ranging from 4.5 to 48 nm and a length of ~1.15 μm [51].

All described studies demonstrated that selected ELP homopolymers can form self-assembled structures in aqueous solutions above their LCST. The diverse self-assembled structures

(e.g., nano- or micro-sized particles or fibers) were constructed by modulating the molecular design parameters of the ELP homopolymers and changing environmental conditions. More intriguing self-assembled structures compared to ELP homopolymers have been produced by designing ELP block copolymers.

2.2. Macromolecular Self-Assembly of ELP-Based Block Copolymers

A block copolymer is a fusion of different types of homopolymers as blocks in the same polymer chain. Two or more ELP homopolymers can be genetically fused and biosynthesized to produce ELP block copolymers. The LCST of various ELP blocks can differ based on the choice of guest residues in the ELP pentapeptide monomers, and this leads to various types of self-assembled nano- and micro-structures based on the solution temperature. Other IDPs, such as the thermoresponsive resilin-like polypeptide (RLP), can be genetically fused as a block with an ELP block. The different thermoresponsive behaviors of both blocks can drive the formation of more complex self-assembled structures compared to block copolymers that are comprised of only ELP blocks. In addition to the intrinsic thermoresponsive responses of those IDPs, the morphology of self-assembled structures can be modulated by molecular design parameters and environmental conditions, such as the overall molar masses of block copolymers, hydrophobicity of blocks, concentrations of block copolymers in solutions, and weight fraction ratios between blocks. For example, the blocks with different degrees of hydrophobicity can self-assemble into a range of structures including micelles [52], vesicles [53] and lamellae [54]. In the following subsections, the design parameters and environmental conditions that control the self-assembled structures with constitutive ELP or ELP-RLP diblock copolymers are discussed.

2.2.1. Self-Assembled Structures from ELP Diblock Copolymers

To fabricate thermoresponsive ELP-based self-assembled structures, Conticello and coworkers designed an ELP diblock copolymer with hydrophilic $[(VPGEG)_1\text{-}(IPGAG)_4]_{14}$ and hydrophobic $[(VPGFG)_1\text{-}(IPGVG)_4]_{16}$ blocks, where the guest residues of the ELP pentapeptide monomers are underlined [55]. When the solution temperature was increased above the LCST of the hydrophobic block, the block became dehydrated and aggregated with the hydrophobic blocks of other ELP block copolymers. This process resulted in a spherical micelle structure with a hydrophobic core and hydrophilic corona. Interestingly, the presence of ionizable glutamic acid

(E) permitted the control of structural size and shape when altering pH because the charge of E can be adjusted, depending on the difference between the solution pH and the isoelectric point of E residues. The pH control led to various self-assembled structures, such as micelles with spherical and cylindrical morphology. Therefore, this study demonstrated that designed ELP block copolymers with charged guest residues can fabricate stimulus-responsive ELP-based self-assembled structures [55].

To explore the self-assembly behaviors of ELP diblock copolymers as a function of concentration in aqueous buffer, Rodríguez-Cabello and coworkers [56] designed ELP diblock copolymers with a hydrophilic block of $[(VPGVG)_2\text{-}VPGEG\text{-}(VPGVG)_2]_{10}$ and a hydrophobic block of $(VGIPG)_{60}$. The thermoresponsive ELP formed spherical micelles above the LCST at concentrations up to 8 mg/mL (Fig 3a and 3e). When the ELP concentration was greater than 8 mg/mL, the size of micelles decreased and cylindrical morphologies were observed (Fig. 3b and 3e), which was explained by the electrostatic repulsion between E residues at the micelle corona region. Below 50 mg/mL, the hydrophobic cores of the small cylindrical micelles subsequently aggregated and formed longer cylindrical micelles due to reduced water availability in the solution that would allow for full hydration of the ELP (Fig. 3e). With further increases in concentration (50 mg/mL), hydrophobic contacts between these aggregated structures acted as an effective cross-linker between the different fibrils and formed fibrillar networks as observed by cryo-electron microscopy (cryoEM) (Fig. 3c and 3e). A further increase in ELP concentration (100 mg/mL) transformed the network into a lyotropic hydrogel, composed of a protein fiber with a hexagonal structure based on small-angle X-ray scattering (SAXS) results (Fig. 3d and 3e). This work successfully demonstrated that altering the concentrations of sequence-controlled ELP diblock copolymers can produce diverse self-assembled structures.

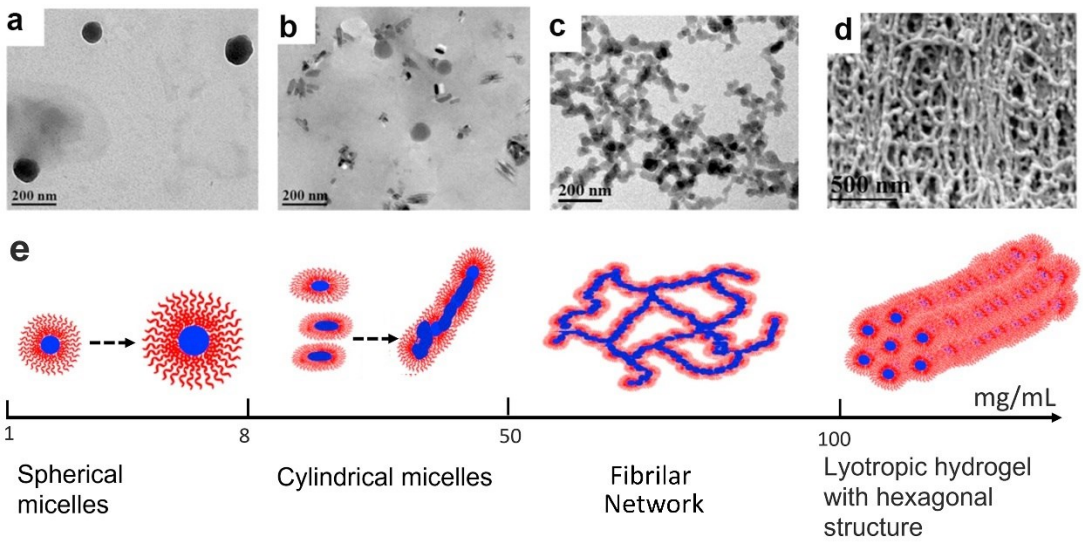

Fig. 3. Morphologies of the self-assembled structures from the ELP diblock copolymers, $[(VPGVG)_2(VPGEG)(VPGVG)_2]_{10}$–$(VPGIG)_{60}$, as a function of concentration in water. (a) Transmission electron microscopy (TEM) images of self-assembled nanoparticles at 1 mg/mL ELP; (b) Cylindrical and spherical morphologies from the ELP self-assembly at 10 mg/mL; (c) CryoEM image of the ELP network at 50 mg/mL; (d) Scanning electron microscope image of the fibrillar ELP structure at 100 mg/mL; (e) Schematic of the morphological transition in a concentration-dependent manner. At 100 mg/mL, lyotropic hydrogels containing hexagonal structures is observed as characterized by small-angle X-ray scattering. The bar representing concentration is not to scale. The blue and red colors represent the hydrophobic block of $(VPGIG)_{60}$ and the hydrophilic block of $[(VPGVG)_2(VPGEG)(VPGVG)_2]_{10}$, respectively. Figure is modified from ref. [56]. Copyright 2015, Elsevier

Molecular design parameters that control the thermoresponsive self-assembly of ELP diblock copolymers were systematically explored by Chilkoti and coworkers [57]. The ELP diblock copolymer was designed with a hydrophilic block of $[(VPG\underline{V}G)_1(VPG\underline{A}G)_8(VPG\underline{G}G)_7]_n$ and a hydrophobic block of $[(VPG\underline{V}G)_5]_n$, resulting in ELP[$V_1A_8G_7$-n]-ELP[$V_5$-n]. The number of blocks, n, were modulated to understand the effects of design parameters, such as molar masses and lengths of block copolymers as well as diverse ratios between the hydrophilic and hydrophobic blocks, on the self-assembled structures. The biosynthesized ELP block copolymers underwent two phase transitions as a function of solution temperature. There was a transition from individual ELP block copolymers (i.e., unimers) to spherical micelles at an intermediate temperature and a

micelle-to-bulk aggregate transition at a higher temperature when the ratio of the hydrophilic block to the hydrophobic block was between 1:2 and 2:1 [57]. However, when the ratio exceeded 2:1, only a single transition from unimers to micron-sized aggregates was observed. This result indicates that a particular range of ratios between ELP blocks can be required to construct self-assembled structures because large hydrophilic blocks in ELP diblock copolymers can prevent structural formation.

By leveraging this discovery, ELP diblock copolymers with two functional peptides were biosynthesized for cancer detection applications. A peptide that is known to target ligands for angiogenic tumor vasculature (green triangle in Fig. 4) was genetically fused to the end of the hydrophilic block, while a peptide that is used as an imaging agent (lightning bolt images in Fig. 4) was attached to the hydrophobic block . ELP diblock copolymers with the attached peptides and various block sizes were biosynthesized, and each block size variant was characterized to identify the unimer-to-spherical micelle transition temperature and the micelle-to-bulk aggregate transition temperature (Fig. 4). The unimer-to-micelle transition temperature was further tuned by controlling the ELP concentrations. The ELP diblock copolymer, ELP[$V_1A_8G_7$-96]-ELP[V_5-60], with tumor-targeting peptides was able to localize on HT 1080 fibrosarcoma cells. Moreover, the ELP was in a unimer state at normal physiological temperature but formed micelles at the tumor site temperature of 42 °C. As a result, the concentrated imaging peptides at the micelle core enhanced the efficiency of tumor detection (Fig. 4). This study presented a method to control self-assembled nanostructures in clinically relevant temperatures by elucidating the sequence-structure-property-performance relationship of designed ELP diblock copolymers. Furthermore, the developed protein polymer was shown to be a viable tool for advanced tumor detection.

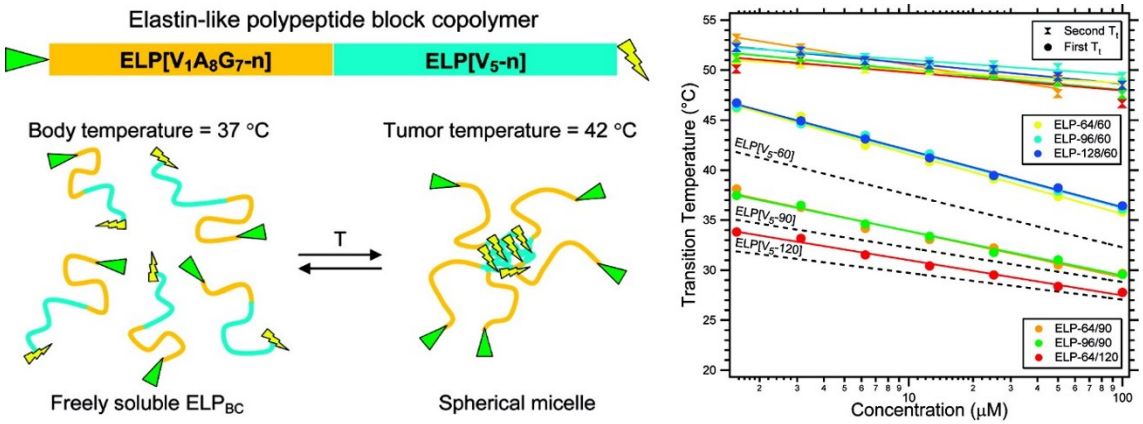

Fig. 4. Design and characterization of temperature-responsive ELP block copolymers with tumor-targeting and imaging peptides. (a) Temperature-triggered self-assembly of ELP diblock copolymers, genetically fused to peptides with the functionalities of tumor recognition and binding (green triangle) and imaging (lightning bolts image). The increased solution temperature initiated self-assembly of the designed protein polymers into multivalent spherical micelles; (b) Transition temperatures (T_t) of ELP micelles as a function of ELP concentration in a physiological buffer. The first T_t is defined as the temperature at the first apparent increase in absorption (filled circles) when measuring optical density at 600 nm as a function of temperature. This indicates a transition from ELP unimers to micelles. The second T_t (filled hourglass) indicates a transition from ELP micelles to bulk aggregation. The figure is adapted from ref. [57]. ACS Publishers Copyright 2008.

Molecular design parameters to construct stable ELP-based self-assembled micelles were investigated by modulating the molar masses of ELP diblock copolymers and elucidating the ranges of weight fraction ratios between the blocks that form micelles [58]. Several designs of ELP diblock copolymers with the sequence of G[(VPG<u>I</u>G)$_m$-(VPG<u>S</u>G)$_n$]Y were produced and had diverse molar masses ranging from 15 kDa to 77 kDa. The shortest diblock copolymer with a 1:1 ratio between hydrophobic and hydrophilic blocks, G[(VPG<u>I</u>G)$_{18}$-(VPG<u>S</u>G)$_{18}$]Y, exhibited only a single unimer-to-bulk aggregate phase transition temperature. The weight fraction ratio of the hydrophilic block to the hydrophobic block was between 1:2 and 2:1 where micelle structures are formed by other ELP diblock copolymers with greater overall molar masses [57]. By increasing the length of the hydrophobic block (VPG<u>I</u>G)$_m$ from m = 18 to m = 24, 36, 48 while maintaining the length of hydrophilic block (VPG<u>S</u>G)$_{n=18}$, dynamic light scattering (DLS) measurements confirmed the presence of unstable self-assembled nanostructures. More stable nanostructures were observed when the hydrophobic block length was greater than 48 (e.g., m = 96). This data and other studies [57] concluded that the careful control of the overall molar mass of the ELP diblock copolymer and the weight fraction ratio of the ELP hydrophobic block to hydrophilic block are critical for the fabrication of self-assembled ELP-based nanostructures with enhanced stability [58].

2.2.2. Self-Assembled Structures from Diblock Copolymers with Constitutive ELP Block and Other Thermoresponsive IDP Blocks

The thermoresponsive ELP diblock copolymer can be engineered by replacing one ELP block with other biosynthetic IDPs for more complex self-assembled structures. Thermoresponsive resilin-like polypeptide (RLP) has been used as a block with ELP in diblock copolymer designs. The repeats of an RLP octapeptide monomer, QYPSDGRG, presented an opposite temperature-triggered phase transition compared to the LCST of ELP, where RLP coacervated below a certain temperature, known as the upper critical solution temperature (UCST) [59]. The combination of LCST and UCST behaviors in the ELP-RLP diblock copolymers further constructed self-assembled structures with more intriguing morphologies than the structures from only ELP diblock copolymers.

The effect of molecular design parameters in ELP-RLP diblock copolymers was thoroughly investigated when constructing self-assembled micelles at solution temperatures below the LCST of ELP and UCST of RLP [60]. Chilkoti and coworkers modulated (i) the size/molar mass of the core-forming hydrophobic RLP block in self-assembled micelle structures, (ii) the molar mass of the hydrophilic ELP block located at corona regions, and (iii) the degree of ELP block hydrophilicity (Table **2**). $(ELP_{Xaa})_n$-RLP_m diblock copolymers were designed and biosynthesized. X_{aa} denotes the guest residue in the typical ELP pentapeptide monomer, while n and m denote the number of the ELP or RLP repeats, respectively. To understand how the molar mass of the hydrophobic RLP block affects the self-assembly of the block copolymer, the number of RLP repeats, m, was increased from 20 to 100, while the number of the $ELP_{A/G}$ repeats, n, was held constant at 80 (Table **2A**). $ELP_{A/G,80}$ was the ELP pentapeptide monomer with A and G as the guest residues at a 1:1 ratio. Although the solution temperature was lower than the UCST of the RLP, RLP_{20}–$ELP_{A/G,80}$ did not construct self-assembled structures. Contrarily, at the same condition, RLP_{40}-$ELP_{A/G,80}$ and RLP_{60}-$ELP_{A/G,80}$ formed self-assembled structures with spherical morphologies of 60-80 nm hydrodynamic diameter. For RLP blocks with greater molar masses, such as RLP_{80}-$ELP_{A/G,80}$ and RLP_{100}-$ELP_{A/G,80}$, self-assembled structures were formed with cylindrical morphologies. This investigation identified that the molar masses of the RLP blocks must be within particular ranges to form self-assembled nanostructures similar to the concept of temperature-triggered, self-assembled structures from ELP diblock copolymers [57] (see section 2.2.1).

Table 2. Self-assembled structures from RLP-ELP diblock copolymers

Design Parameters at Molecular Level	RLP-ELP[1] Diblock Copolymer	Self-Assembled Structure[2]
A. Size/molar mass of the hydrophobic RLP block	RLP_{20}–$ELP_{A/G,80}$	No self-assembly
	RLP_{40}–$ELP_{A/G,80}$	Spherical micelle
	RLP_{60}–$ELP_{A/G,80}$	Spherical micelle
	RLP_{80}–$ELP_{A/G,80}$	Cylindrical micelle
	RLP_{100}–$ELP_{A/G,80}$	Cylindrical micelle
B. Molar mass of the hydrophilic ELP block	RLP_{40}–$ELP_{A/G,40}$	Cylindrical micelle
	RLP_{40}–$ELP_{A/G,80}$	Spherical micelle
	RLP_{40}–$ELP_{A/G,160}$	Spherical micelle
	RLP_{80}–$ELP_{A/G,80}$	Cylindrical micelle
	RLP_{80}–$ELP_{A/G,160}$	Spherical micelle
C. Modulated hydrophilicity of the ELP block in RLP-ELP block copolymer	RLP_{40}–$ELP_{S,80}$	Spherical micelle
	RLP_{40}–$ELP_{A/G,80}$	Spherical micelle
	RLP_{40}–$ELP_{V,80}$	Cylindrical micelle
	RLP_{80}–$ELP_{S,80}$	Spherical micelle
	RLP_{80}–$ELP_{A/G,80}$	Cylindrical micelle
	RLP_{80}–$ELP_{V,80}$	Cylindrical micelle

[1] RLP_m = $(QYPSDGRG)_m$; $ELP_{A/G,n}$ $[(\underline{A/G})GVPG]_n$= ; $ELP_{S,n}$ = $(\underline{S}GVPG)_n$; $ELP_{V,n}$ = $(\underline{V}GVPG)_n$

[2] Solution temperature was set to 15 °C. The temperature was below the LCST of ELP blocks and the UCST of RLP blocks in RLP-ELP diblock copolymers. In this condition, RLP constructed the core of spherical or cylindrical micelles

To establish the relationship between the molar masses of hydrophilic ELP blocks and the self-assembly of ELP-RLP diblock copolymers, the molar masses of $ELP_{A/G,n}$ blocks were varied while the RLP repeats were maintained with m=40 or m=80, $RLP_{40,80}$-$ELP_{A/G,n}$ (Table 2B). Under the UCST of the RLP block, RLP_{40}-$ELP_{A/G,40}$ and RLP_{80}-$ELP_{A/G,80}$ self-assembled into cylindrical micelles. When the weight fraction of the hydrophilic ELP block was greater than the RLP block, such as RLP_{40}-$ELP_{A/G,80}$, RLP_{40}-$ELP_{A/G,160}$, and RLP_{80}-$ELP_{A/G,160}$, the structure changed from cylindrical to spherical. These results indicate that the self-assembled RLP-ELP micelle structures can be cylindrical or spherical depending on whether the weight fraction of the RLP block or ELP block is greater, respectively. In addition, it is interesting to note that the overall molar masses of the diblock copolymers are critical for self-assembly because RLP_{20}–$ELP_{A/G,80}$ did not form any structures despite having the same ratio of block weight fractions as RLP_{40}-$ELP_{A/G,160}$, which formed spherical micelles. In summary, the tested RLP-ELP diblock copolymers showed that the ratio of weight fractions between the RLP and ELP blocks and the minimum RLP repeats (e.g.,

m=40 when n = 40 and 80 in RLP_m-$ELP_{A/G,n}$ block) are critical to form self-assembled structures at solution temperatures under the LCST and UCST of the ELP and RLP blocks, respectively.

The degree of ELP block hydrophilicity within the RLP-ELP diblock copolymers were modulated by altering the guest residues, and effects on the self-assembled structures were investigated. A/G guest residues in the ELP block of RLP_{40}-$ELP_{A/G,80}$ and RLP_{80}-$ELP_{A/G,80}$ were replaced with S (more hydrophilic) or V (more hydrophobic) residues (Table 2C). Below the UCST and LCST of the RLP and ELP blocks, respectively, self-assembled spherical micelle structures were observed from both RLP_{40}-$ELP_{A/G,80}$ and the more hydrophilic RLP_{40}-$ELP_{S,80}$. Cylindrical micelles were detected when the S guest residue in ELP was replaced with the more hydrophobic V, RLP_{40}-$ELP_{V,80}$, and when the weight fraction of RLP was increased, RLP_{80}-$ELP_{A/G,80}$. However, while maintaining the high RLP weight fraction and with hydrophilic S as the ELP guest residue, RLP_{80}-$ELP_{S,80}$, spherical micelle structures were observed. These results indicate that when the weight fraction of $ELP_{A/G}$ is smaller than RLP in RLP-$ELP_{A/G}$ block copolymers, self-assembled cylindrical micelle structures are often constructed rather than the spherical structures (Table 2). However, by controlling the hydrophilicity of the ELP block, the morphology of self-assembled structures with constitutive ELP-RLP diblock copolymers can be tailored at solution temperature ranges below the UCST of the RLP block and below the LCST of the ELP block. The discovery of diverse molecular design parameters in ELP-RLP diblock copolymers, such as overall molar masses, the ratio of weight fractions between the blocks, and the degree of hydrophilicity, expands the library of the ELP-based block copolymers that allow for the construction of targeted self-assembled nanoscale morphologies.

The self-assembly behaviors of the same set of the RLP-ELP diblock copolymers, G-$(QYPSDGRG)_m$-$[(\underline{A}/\underline{G})GVPG]_{80}$ where m=20, 40, 60, 80 and 100, were further investigated in more highly concentrated solutions (i.e., 30 wt% and 50 wt%) [61]. In block copolymer systems, self-assembled structures typically have a stronger dependence on the molar mass ratios of the various blocks compared to the solution temperature [61]. These systematic tests ascertained how changes to the molar masses of the RLP blocks affected the self-assembly of RLP-ELP diblock copolymers. Moreover, both RLP and ELP have temperature-responsive behaviors in solutions; thus, the impact of temperature on the self-assembly was evaluated from 10 ^oC to 45 ^oC. SAXS detected that ELP-RLP polymers self-assembled into hexagonally packed cylinders (HPC) or lamellae (LAM) structures when the molar masses of the RLP block were above particular RLP

volume fraction thresholds and the solution temperature was under the RLP UCST (i.e., 50 ºC) and ELP LCST (i.e., 20-25 ºC) within the tested conditions for 30 and 50 wt%), where RLP blocks aggregate but ELP remains soluble (Fig. 5a). However, disordered structures were observed when the molar masses of the RLP blocks were under the threshold, regardless of temperature and concentration. In addition, self-assembled HPC or LAM structures switched to disordered structures when the solution temperature was increased above the LCST of the ELP blocks, which implies a significant alteration in the interaction between the ELP and water. At a solution concentration of 50 wt%, disordered or LAM structures were observed when molar masses of the RLP block and solution temperatures were controlled, but hexagonally packed cylindrical structures were not observed for RLP-ELP polymers, even when the RLP block volume fraction was greater than 0.7 (Fig. 5b). This work demonstrated that modulating design parameters of thermoresponsive RLP-ELP diblock copolymers as well as controlling environmental parameters (e.g., highly concentrated polymers in solution) can construct diverse self-assembled structures from nanoscale (Table 2) to larger constructs.

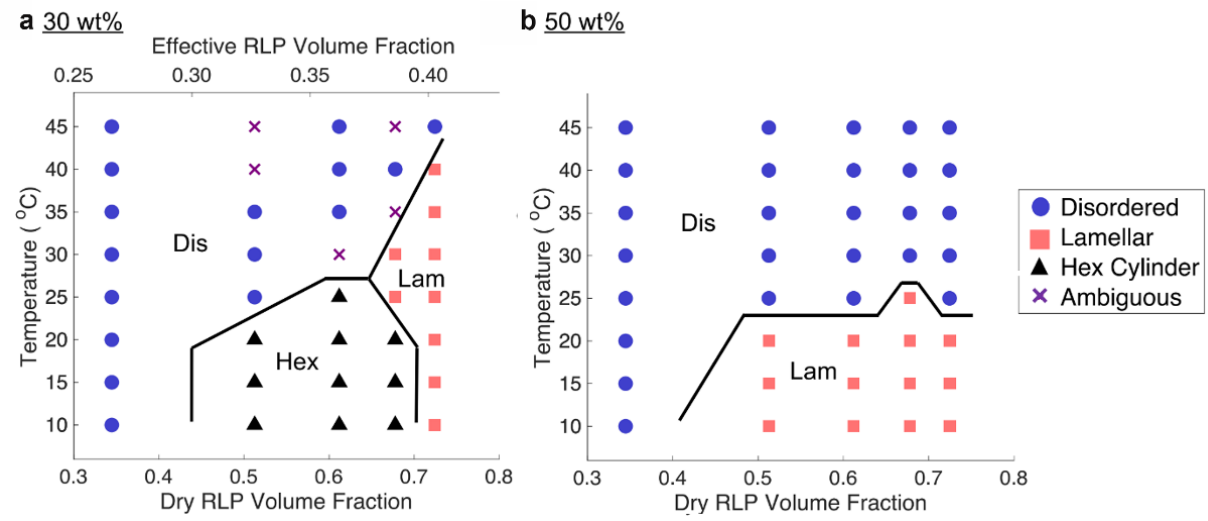

Fig. 5. Phase diagram of $RLP_{m=20,40,60,80,100}$-ELP_{80} diblock copolymers at 30 wt% (a) and 50 wt% (b) in aqueous solutions. Three main phases were described as disordered (Dis, blue solid circle), lamellar (Lam, red solid square), hexagonally packed cylindrical (Hex, black solid triangle), or ambiguous (X) phases based on SAXS data. The figure is adapted from ref [61]. ACS Publishers. Copyright 2021.

Lim and coworkers captured the dynamic self-assembly of ELP-RLP block copolymers by modulating solution temperatures [62]. RLP (R) and ELP (E) monomers were designed with an equal number of amino acids, and the monomers were repeated, E_mR_n, to produce diblock copolymers (Fig. 6a). The diblock copolymers self-assembled into vesicles with lipid-bilayer shapes when the solution temperature was below both the LCST of the E_m block and the UCST of the R_n block, and the molar masses of R_n block were similar to or slightly greater than the E_m block (i.e., m=6 and n=6 or greater). The R_n blocks were located inside the vesicles due to hydrophobic interactions, and the E_m blocks were outside the vesicles for increased water contact (Fig. 6b). When the molar mass of the E_6 block was doubled, E_{12}, and genetically fused with R_{24} block and biosynthesized, the diblock copolymers transformed into micelles with an R_{24} core and E_{12} corona because R blocks coacervate below their UCST while E blocks are soluble under their LCST (Fig. 6b). Conversely, when the solution temperature was increased above both the LCST and UCST, all E_mR_n block copolymers transformed into micelles where the E_m block was at the core and R_n block was at the corona regardless of whether the molar mass of the E_m block was greater or less than the R_n block. This is caused by the coacervation of the E_m block above its LCST while the R_n block is soluble above its UCST (Fig. 6b). As expected, the block copolymers only fully coacervated or aggregated when the solution temperature was above the LCST and below the UCST.

This finding can potentially lead to the design of an ELP-RLP diblock copolymer with the ELP LCST around 40 °C and the RLP UCST fitting into a narrow temperature range (i.e., 37~40 °C. By incorporating peptides that target cancer cells into the ELP blocks and packaging anticancer drugs into the RLP cores at 37 °C, the self-assembled micelle structures can target tumor sites at body temperature due to the location of the peptides on the ELP corona. The increased temperatures at the tumor sites (approximately 42 °C) can transform the position of the RLP block from the core to the corona in the micelle structure (Fig. 6b), and the transformation can release a drug in the target cancerous location. It is expected that the development of the thermoresponsive ELP-RLP diblock copolymers will contribute to the field of targeted therapeutic delivery.

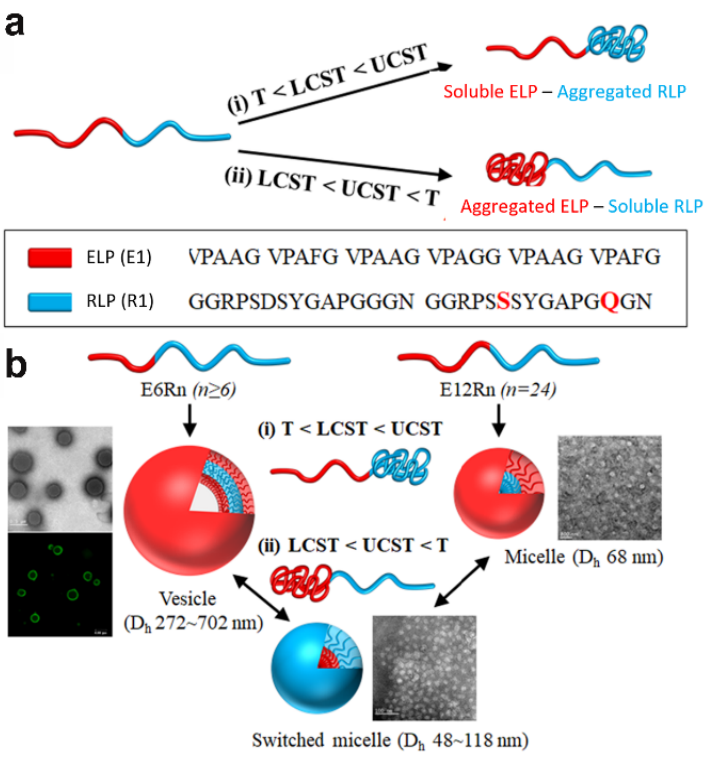

Fig. 6. Design of ELP-RLP diblock copolymers to form dynamic self-assembled structures using thermoresponsive inverse phase transition behaviors of each block. (a) Expected ELP-RLP diblock copolymer behaviors depending on solution temperatures. Protein sequences of ELP and RLP blocks that have the same numbers of amino acids. (b) Schematics of dynamic nanostructures of ELP−RLP diblock copolymers at the solution temperature below and above the ELP LCST and RLP UCST. D_h denotes the hydrodynamic diameter of detected particles. This figure is adapted from ref. [62]. ACS Publishers. Copyright 2021.

Instead of RLP blocks in the RLP-ELP diblock copolymers, silk-like polypeptides (SLPs) have been used to prepare SLP-ELP (SELP) diblock copolymers. Among the major benefits of SLP blocks are the enhanced mechanical properties and stability of SELP materials; thus, SELP diblock copolymers are discussed in section 6.

2.3. Self-assembled Structures from ELP-based Polymer Hybrids Containing Functional (Bio)molecules

The main driving force behind the self-assembly of ELP homopolymers and ELP-based diblock copolymers is coacervation, which occurs at solution temperatures greater than the LCST

of the ELP. However, ELPs with a molar mass below a particular threshold can have LCSTs that are too high such that their phase transition behaviors cannot be observed at high solution temperatures. To observe the coacervation behavior and potentially promote the self-assembly of ELPs with low molar masses, conjugations of self-assembling small molecules to ELPs were introduced. This approach increases the quantity of ELPs in self-assembled structures, which sufficiently decreases the ELP LCSTs to fabricate thermoresponsive, self-assembled structures. The Kiick group [63] chemically conjugated triple-helix-forming collagen-like peptides (CLPs) to low molar mass ELPs, $(VPG\underline{F}G)_6$. The initial molecular self-assembly of CLPs into triple helices in solution prepared ELP-CLP trimeric structures. ELP-CLP trimers formed well-defined, stable vesicles with hydrodynamic diameters that ranged from approximately 30 to 200 nm within a temperature range from 4 °C to 65 °C, where the diameters tended to increase with temperature. Nanospheres were also formed by conjugating low molecular weight $(VPG\underline{F}G)_6$ ELPs with oligonucleotides, exploiting DNA base-pairing for molecular self-assembly. The LCSTs decreased with increasing quantities of ELPs in ELP-oligonucleotide nanospheres, and the sizes of nanospheres were tunable depending on the solution temperature [64]. Furthermore, MacKay and coworkers identified that the conjugation of two saturated 16-carbon chains (C16) to each ELP $(VPG\underline{A}G)_3$ enabled ELP phase separation to occur at temperatures similar to their greater molar mass counterparts [65]. TEM captured that ELP-C16 self-assembled into long cylindrical micelles of 1.7 ± 0.2 μm in length and 16.0 ± 2.0 nm in diameter. The conjugation of other molecules that are capable of molecular self-assembly provides additional opportunities for ELPs with small molar masses, which are generally not capable of self-assembly on their own, to form temperature-triggered, self-assembled structures.

Although many ELP homopolymers coacervate above their LCST without forming self-assembled structures, the conjugation of small molecules to ELP homopolymers can promote self-assembly [18, 66, 67]. ELP homopolymers that transform from unimers to aggregates above their LCSTs can switch into nanoparticles when chemical compounds with specific hydrophobicity indices are covalently attached [68]. When the octanol-water distribution coefficients of attached chemical compounds were greater than 1.5, the ELP-compound fusions self-assembled into sub-100 nm nanoparticles that were stable at low-micromolar concentrations in aqueous solutions above their LCSTs [68]. The stability of the nanoparticles at suitable concentrations is required for

drug delivery applications, and the revealed characteristics make ELP-compound fusions good candidates for practical utilization in nanomedicine.

ELP homopolymers have been genetically fused to structured proteins or peptides to prepare self-assembled nanostructured materials with new or improved functionalities. Olsen and coworkers investigated self-assembly behaviors of ELP-globular mCherry protein block copolymers [67, 69, 70]. A systematic study of mCherry-ELP diblock copolymers showed diverse self-assembled nanostructured materials that depend on the protein concentration, volume fractions of protein blocks, and solution temperatures. Since mCherry is used as a model for functional globular proteins such as enzymes, globular protein-ELP fusion technology demonstrates the potential for well-organized enzymes in nanostructured materials, guided by the self-assembly behaviors of ELP blocks. This approach is expected to improve the functionalities of enzymes embedded in materials (e.g., thin films) compared to conventional materials where enzymes are randomly distributed and oriented [71].

Rodríguez-Cabello and coworkers investigated the self-assembly behaviors of ELP diblock copolymers that were genetically fused with self-assembling antimicrobial peptides (AMPs) [18]. The ELP design was composed of a hydrophilic $(VPG\underline{S}G)_{50}$ block and a hydrophobic $(IPG\underline{V}G)_{60}$ block (guest residues are underlined). The self-assembling AMPs, GL13K and 1018, were genetically fused to the hydrophilic ELP block. At 37 °C, the ELPs self-assembled into micelles with the hydrophobic block at the core and the hydrophilic block at the corona, such that the AMPs were located on the outer surface of the corona. When switching to a basic solution, nanofibers with lengths of 27.0±16.5 nm and 118.2±68.6 nm in the GL13K-ELP and 1018-ELP samples were observed, respectively. Both AMPs were able to cause the formation of nanofibers because GL13K self-assembles into defined twisted nanoribbons [66], and 1018 aggregates into non-defined, polydisperse nanostructures [72] without ELP. When the samples were stored in the solution for more than a week, the nanofiber sizes of GL13K-ELP and 1018-ELP increased to 314.7±220.8 nm and 506.6±425.9 nm, respectively. These large nanofibers were not observed in the absence of AMPs. Therefore, this study serves as an example of ELP-based biomolecular hybrids for the development of diverse self-assembled nanostructured materials.

3. Stability of Self-Assembled IDP Structures

The main driving force of self-assembled structures are non-covalent interactions, such as hydrogen bonds, and hydrophobic interactions [73]. The structures are formed without the intervention of any catalyst or activator, and the interactions between the polymer components determine the size and shape of the structures [74]. A major advantage of IDP self-assembly is their ability to construct dynamic structures that respond to changes in environmental conditions (e.g., Fig. 1c and 6). However, this advantage is also a major challenge when it is necessary to maintain the specific self-assembled structures across various external conditions. For example, self-assembled micelles at body temperature using designed ELP diblock copolymers can be utilized for drug delivery applications. Yet, micelle stability for drug delivery is critical to prevent unintentional nanostructure disassembly in diluted environments and dynamic blood flows. Efforts to enhance the stability of self-assembled IDP-based structures include controlling the size of the hydrophobic block in hydrophobic-hydrophilic diblock copolymers, embedding mechanically stable sequences in IDPs, forming IDP-composite nanostructures, and genetically engineering IDPs with natural and unnatural amino acids to chemically crosslink the self-assembled structures (Fig. 1d).

The stability of self-assembled structures, such as micelles, from ELP diblock copolymers with constitutive hydrophobic and hydrophilic ELP blocks depends on the size of the hydrophobic block [58]. ELP diblock copolymers were synthesized with the sequence $(VPGSG)_m$-$(VPGIG)_n$ where m and n were either 18, 24, 36, 48, or 96. Out of these diblock copolymers, stable micelles were formed when the size of the hydrophobic block n was greater than 48 (Fig. 7a). Intermediate nanostructures were constructed when n was less than 48, which showed instability over the period of dynamic light scattering measurements. This indicates that minimum sizes of the hydrophobic blocks in hydrophobic-hydrophilic diblock copolymers need to be identified to construct stable self-assembled micelles.

The use of mechanically stable peptides or proteins as monomers or blocks improved the mechanical stability of self-assembled IDP-based nanostructures. The hexapeptide GAGAGS from the Bombyx mori silk moth was incorporated with ELP pentapeptide monomer sequences to form various silk–elastin-like polypeptide (SELP) alternating copolymers, $[(GVGVP)_4(GYGVP)(GVGVP)_3$-$(GAGAGS)_{n=1,2,4}]_{m=9,12,14}$ [75-77]. A two-step self-assembly was detected when SELP was in aqueous solution and the temperature was modulated. SELP spontaneously self-assembled into micellar-like structures due to hydrophobic interactions and

hydrogen bonding within the silk domains. Different self-assembled structures formed when the solution temperature was greater than the LCST of the ELP sequences. At this stage, various nanostructures, such as nanoparticles, nanofibers, and hydrogel particles, were reversibly or irreversibly constructed depending on the weight fractions between the ELP and silk blocks in SELP (Fig. 7b) [78]. A further study of self-assembled SELP nanoparticles identified that intermolecular hydrogen bonding between silk blocks physically form beta-sheets and construct concentration-dependent SELP-based protein networks and nanogels in aqueous solutions [79]. SEM imaging of lyophilized SELP revealed globular particle formation within various concentration ranges, indicative of self-assembly. The nanostructures were stable when diluted, indicating hydrophobic interactions were not the only parameter for stability. In addition, three SELP polymers were synthesized for a different study with various silk to ELP block ratios of 1:8, 1:4, and 1:2, respectively. At these ratios, the SELP spontaneously, or by thermal triggering, self-assembled into micellar-like nanoparticles either reversibly or irreversibly [77]. The stability of the SELP nanoparticles were evaluated via loading of hydrophobic antitumor drugs, such as doxorubicin. It was revealed that the doxorubicin-loaded SELP-based nanoparticles were stable even after 48 hours despite the low protein polymer concentration of 1 mg/mL [80]. Therefore, incorporating mechanically stable peptides or proteins in IDP-based polymers can be considered a promising approach to improve the stability of IDP-based self-assembled structures. More detailed applications of SELP for drug delivery and tissue engineering can be found elsewhere [75].

ELP was further engineered to improve the stability of ELP-based self-assembled structures by incorporating specific natural and unnatural amino acids that can be crosslinked via covalent bonds. It has been demonstrated that the guest residues in the ELP pentapeptide monomer can be filled with natural amino acids, such as Y and L, as chemical crosslinking sites [81-83], including photo-crosslinking (Fig. 7c) [84, 85], to stabilize ELP-based self-assembled structures. Moreover, unnatural amino acids, such as para-azidophenylalanine (pAzF), have been incorporated in ELP to photo-crosslink specific unnatural amino acid residues (Fig. 7d) [8, 86].

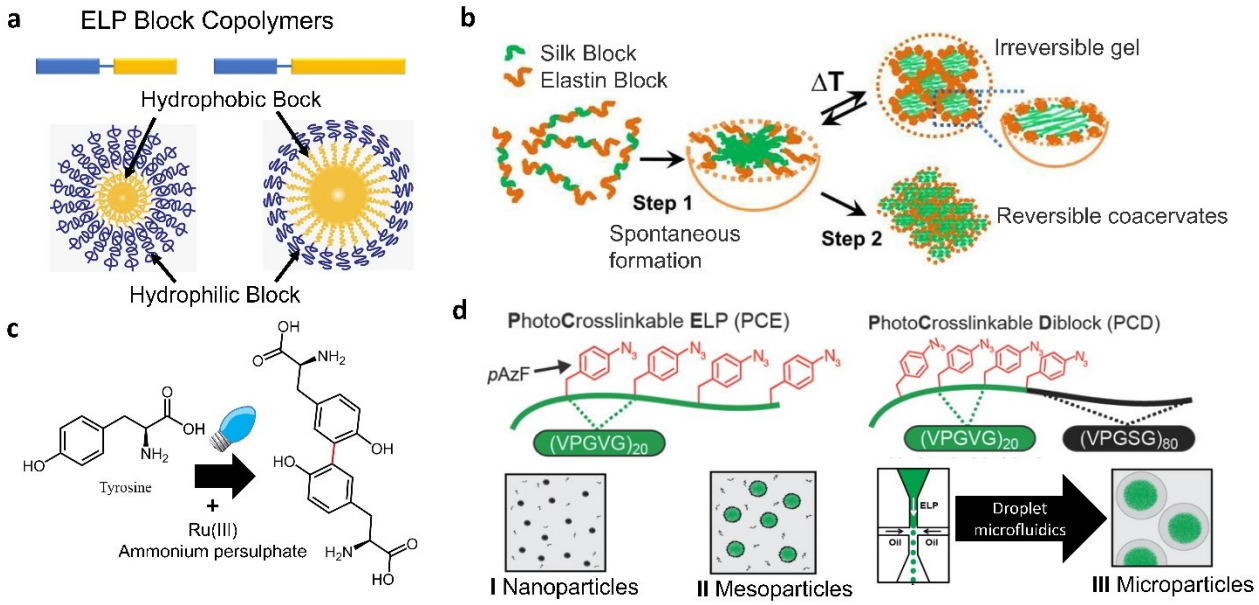

Fig. 7. Diverse methods to reinforce self-assembled IDP structures. (a) Optimal range of hydrophobic block lengths in IDP-based block copolymers; (b) Use of mechanically stable blocks such as silk-like polypeptides, adapted from ref. [77] ACS publications, Copyright 2011; (c) Crosslinking of naturally occurring amino acids in biosynthetic IDPs and (d) Crosslinking unnatural amino acids in IDP homopolymers and block copolymers. This figure is modified from ref. [8]. Wiley Online Library, Copyright 2018

By incorporating photo-crosslinkable unnatural amino acids in ELP-based polymers, the self-assembly behavior of the ELP and the stability of the photo-crosslinked, self-assembled structures were investigated [8]. A photo-crosslinkable ELP (PCE) was engineered by adding four regularly spaced unnatural amino acids, such as pAzF, in the ELP homopolymer $(VPG\underline{V}G)_{80}$. In addition, a photo-crosslinkable diblock (PCD) copolymer was designed via genetically fusing a PCE block with a hydrophilic ELP block (Fig. 7d) [8]. Raising the solution temperature triggered the self-assembly of PCD copolymers into nanoscopic, spherical micelles (Fig. 7d-I) with a PCE core and a hydrophilic ELP corona. Ultraviolet irradiation activated the aryl azide group on the pAzF residues and formed a reactive nitrene, which then crosslinked with nearby N-H or C-H bonds. The photo-crosslinking process stabilized the PCE core in self-assembled PCD micelles. The crosslinked micelles demonstrated reversible thermoresponsive behaviors by shrinking upon heating as the hydrophobic core desolvated and swelled upon cooling without disassembling, unlike other self-assembled ELP micelles that are prepared without crosslinking [8].

On the contrary, PCE or the mixture of PCD and PCE resulted in microscopic or mesoscopic particles, respectively, where the particles were stabilized by the photo-crosslinking process (Fig. 7d-II). In the mixture, mesoscopic particles were constructed by increasing the solution temperature above the LCST or phase-transition temperature of PCE and the micelle temperature of PCD. The particle sizes ranged from 100 nm to 1 μm and were tuned by the mixture ratio between PCE and PCD. The photo-crosslinking process generated covalent bonds within the particles and stabilized the morphology of the self-assembled structures. Without PCD, microfluidic chips were used to fabricate monodisperse water-in-oil droplets that contained only PCE. At temperatures above the phase-transition temperature of PCE, microscopic particles were formed (Fig. 7d-III) and photo-crosslinked. The initial PCE concentrations controlled the sizes of microparticles, and the photo-crosslinking stabilized the particles such that the lyophilized particles were able to recover their microdroplet structure in solution and maintain their structural integrity and sizes at various temperatures for more than a week. This study demonstrated an excellent method to stabilize self-assembled, thermoresponsive ELP structures, as well as to control their sizes.

To stabilize self-assembled ELP structures, diverse approaches beyond biomolecular engineering and biosynthesis have been attempted. For example, stable ELP-based self-assembled nanostructures were constructed by synthesizing poly(N-3-acrylamidophenylboronic acid), PAPBA, in the presence of ELP, resulting in phenylboronic acid-incorporated ELP spherical nanoparticles [87]. The ELP-based composite nanoparticles had diameters of approximately 100 nm and were shown to be stable across a wide pH range (i.e., pH 3~9) due to interactions between the boronic acid group of phenylboronic acid in PAPBA and the basic groups of ELP via the Lewis acid–base reaction.

The progress in IDP self-assembly clearly shows not only the formation of dynamic and stimulus-responsive self-assembled structures but also self-assembled structures that are stable against various environmental conditions. It is expected that these molecular design approaches and various materials processing techniques will expand the utilization of the engineered IDPs for advanced biotechnology applications.

4. Summary and Outlook

The study of self-assembled structures from engineered intrinsically disordered protein (IDP) polymers has largely expanded in the last few decades with the discovery of diverse biosynthetic IDPs. Genetic engineering allows for the precise control of design parameters, such as sequences, molar mass, and weight fraction ratios between blocks in IDP polymers. Biosynthesis guarantees the reproducibility of designed IDP polymers, such as ELP homopolymers, ELP-based diblock copolymers, and ELP-based polymer hybrids containing functional (bio)molecules. Not only controlling diverse design parameters of IDP polymers but also modulating environmental conditions (e.g., solution temperatures, protein and salt concentrations) have led to well-controlled, dynamic, self-assembled IDP polymer structures with a range of nanoscale to larger sizes. The dynamic self-assembled structures have been extensively used for a variety of biomedical applications, including nanomedicine and tissue engineering [13, 14]. To overcome challenges when applying self-assembled structures, such as unexpected drug release, and degradation of structural components, approaches to enhance the stability of the self-assembled IDP-based polymer structures have been developed as reviewed in this article. In addition, as reviewed elsewhere [88], exploiting dynamic covalent bond chemistries, such as Schiff base, hydrazone, oxime, disulfide, and Diels-Alder, allow for both enhanced bond strength and self-healing functionalities within engineered hydrogel tissue structures for long-term tissue engineering and cell culture studies. It is anticipated that developed approaches to enhance the stability of self-assembled structures will advance technologies for additional biomedical applications where structural stability is critical.

The main purpose for the development of IDP-based self-assembled materials is for future industrial applications in diverse fields, especially technologies within healthcare. To translate IDP-based self-assembled materials into commercialized products, several factors need to be addressed, such as protein polymer yields, sustainability, biocompatibility, and diverse functional applications. The yields of biosynthetic IDPs, specifically ELPs, are typically reasonable for biomanufacturing, > 200~300 mg from 1L cell culture [85]. However, the synthesis of ELPs genetically fused with other peptides or IDP blocks can have dramatically lower yields. It will be critical for commercialization to optimize the biosynthesis of the IDP polymers such that yields are consistently high. There are many current research projects focusing on the conversion of raw materials into sustainable industrial products [20, 89], and ELP-based polymeric materials would be an ideal candidate for this purpose. Biosynthesis technologies exploit the stability of DNA and

genetically transformed cells when stored at -80 °C. An arbitrarily large amount of IDP polymers can be biosynthesized from a trivial amount of cell stock because cells grow exponentially in growth media with the appropriate environmental conditions, and cell cultures can always be saved as additional frozen cell stocks. ELP, and IDP-based self-assembled structures in general, are known for non- or low-immunogenic profiles [5-8] and have been tested successfully *in vivo* [90-92]. However, it is difficult to determine whether all current and future biosynthetic IDP-based self-assembled structures are also biocompatible. The development of simplified yet effective processing for biocompatibility testing will reduce the translational time from the bench to the bedside. Although IDP-based self-assembled structures with diverse functionalities are unlimited, only a few types of biosynthetic IDPs are widely available, such as ELP, SLP, RLP; thus, their functionalities are currently limited. Since more biosynthetic IDPs are in the pipeline, for example selective filtering nucleoporin-like polypeptides (NLP) [93, 94], novel biosynthetic IDPs as building blocks for precisely engineered IDP polymers are expected to open new opportunities for advanced biotechnology.

Declaration of Competing Interest

The authors declare that they have no known competing financial interests or personal relationships that could have appeared to influence the work reported in this paper.

Acknowledgement

We are grateful for our support from the Technology and Research Initiative Fund (TRIF) from Arizona for Improving Health and in part by the NSF CAREER grant (DMR-2143126).

References

1. Dyson, H.J. and P.E. Wright, *Intrinsically unstructured proteins and their functions.* Nature reviews molecular cell biology 2005. **6**: p. 197-208.
2. Tompa, P., *Intrinsically unstructured proteins.* Trends Biochem Sci., 2002. **27**(10): p. 527-533.
3. Meyer, D.E. and A. Chilkoti, *Purification of recombinant proteins by fusion with thermally-responsive polypeptides.* Nat Biotechnol., 1999 **7**(11): p. 1112-1115.
4. Banki, M.R., L. Feng, and D.W. Wood, *Simple bioseparations using self-cleaving elastin-like polypeptide tags.* Nat. Methods, 2005. **2**: p. 659-661.
5. Floss, D.M., et al., *Expression and immunogenicity of the mycobacterial Ag85B/ESAT-6 antigens produced in transgenic plants by elastin-like peptide fusion strategy.* J Biomed Biotechnol., 2010. **2010**: p. 274346.
6. Le, D.H.T. and A. Sugawara-Narutaki, *Elastin-like polypeptides as building motifs toward designing functional nanobiomaterials.* Molecular Systems Design & Engineering, 2019. **4**(3): p. 545-565.
7. Roberts, S., et al., *Injectable tissue integrating networks from recombinant polypeptides with tunable order.* Nat Mater., 2018. **17**(12): p. 1154-1163.
8. Costa, C.A., et al., *Photo-Crosslinkable Unnatural Amino Acids Enable Facile Synthesis of Thermoresponsive Nano- to Microgels of Intrinsically Disordered Polypeptides.* Advanced Materials, 2018. **30**: p. 1704878.
9. Rodríguez-Cabello, J.C., et al., *Elastin-like polypeptides in drug delivery.* Advanced Drug Delivery Reviews, 2016. **97**: p. 85-100.
10. MacEwan, S. and A. Chilkoti, *Applications of elastin-like polypeptides in drug delivery.* J Control Release, 2014. **190**: p. 314-330.
11. Massodi, I., G.L. Bidwell III, and D. Raucher, *Evaluation of cell penetrating peptides fused to elastin-like polypeptide for drug delivery.* Journal of Controlled Release, 2005. **108**(2): p. 396-408.
12. Cho, S., et al., *Immune-tolerant elastin-like polypeptides (iTEPs) and their application as CTL vaccine carriers.* J Drug Target, 2015. **24**(4): p. 328-339.

13. Sani, E.S., et al., *Engineering Adhesive and Antimicrobial Hyaluronic Acid/Elastin-like Polypeptide Hybrid Hydrogels for Tissue Engineering Applications.* ACS Biomater. Sci. Eng., 2018. **4**(7): p. 2528-2540.
14. Fernández-Colino, A., et al., *Macroporous click-elastin-like hydrogels for tissue engineering applications.* Materials Science and Engineering: C, 2018. **88**: p. 140-147.
15. Atefyekta, S., et al., *Antibiofilm elastin-like polypeptide coatings: functionality, stability, and selectivity.* Acta Biomaterialia, 2019. **83**: p. 245-256.
16. Ingrole, R.S., et al., *Synthesis and Immunogenicity Assessment of Elastin-Like Polypeptide-M2e Construct as an Influenza Antigen.* Nano Life, 2014. **4**(2): p. 1450004.
17. Costa, A., et al., *Development of Elastin-Like Recombinamer Films with Antimicrobial Activity.* Biomacromolecules, 2015. **16**(2): p. 625-635.
18. Acosta, S., et al., *Dual Self-Assembled Nanostructures from Intrinsically Disordered Protein Polymers with LCST Behavior and Antimicrobial Peptides.* Biomacromolecules, 2020. **21**: p. 4043–4052.
19. Saha, S., et al., *Engineering the Architecture of Elastin-Like Polypeptides: From Unimers to Hierarchical Self-Assembly.* Adv. Ther. , 2020. **3**: p. 1900164.
20. Lima, L.F., et al., *Elastin-like Polypeptides in Development of Nanomaterials for Application in the Medical Field.* Frontiers in Nanotechnology, 2022. **4**: p. 874790.
21. Rodríguez-Cabello, J.C., et al., *Nanotechnological Approaches to Therapeutic Delivery Using Elastin-Like Recombinamers.* Bioconjugate Chemistry, 2015. **26**: p. 1252-1265.
22. Smits, F.C.M., et al., *Elastin-Like Polypeptide Based Nanoparticles: Design Rationale Toward Nanomedicine.* Macromol Biosci., 2014. **15**: p. 36-51.
23. Navon, Y. and R. Bitton, *Elastin-Like Peptides (ELPs) – Building Blocks for Stimuli-Responsive Self-Assembled Materials.* Israel Journal of Chemistry, 2016. **56**(8): p. 581-589.
24. Kim, T.G., H. Shin, and D.W. Lim, *Biomimetic Scaffolds for Tissue Engineering.* Advanced functional materials, 2012. **22**(12): p. 2446-2468.
25. Baldock, C., et al., *Shape of tropoelastin, the highly extensible protein that controls human tissue elasticity.* Proceedings of the National Academy of Sciences, 2011. **108**: p. 4322–4327.

26. Urry, D.W., C.H. Luan, and S.Q. Peng, *Molecular biophysics of elastin structure, function and pathology*, in *Ciba Foundation symposium*. 1995, John Wiley & Sons. p. 4-22.
27. Roberts, S., M. Dzuricky, and A. Chilkoti, *Elastin-like polypeptides as models of intrinsically disordered proteins.* FEBS letters, 2015. **589(19 Pt A)**: p. 2477–2486.
28. Urry, D.W., *Molecular Machines: How Motion and Other Functions of Living Organisms Can Result from Reversible Chemical Changes.* Angewandte Chemie, 1993. **32**(6): p. 819-841.
29. Wright, E.R. and V.P. Conticello, *Self-assembly of block copolymers derived from elastin-mimetic polypeptide sequences.* Adv Drug Deliv Rev, 2002. **54**(8): p. 1057-1073.
30. Glassman, M.J. and B.D. Olsen, *End Block Design Modulates the Assembly and Mechanics of Thermoresponsive, Dual-Associative Protein Hydrogels.* Macromolecules, 2015. **48**: p. 1832-1842.
31. Martino, M. and A.M. Tamburro, *Chemical synthesis of cross-linked poly(KGGVG), an elastin-like biopolymer.* Biopolymers 2001. **59**: p. 29–37.
32. Flamia, R., et al., *AFM study of the elastin-like biopolymer poly(ValGlyGlyVal-Gly).* Biomacromolecules, 2004. **5**: p. 1511–1518.
33. Flamia, R., et al., *Transformation of amyloid-like fibers, formed from an elastinbased.* Biomacromolecules, 2007. **8**: p. 128-38.
34. Swierczewska M, et al., *Cellular response tonanoscale elastin-like polypeptide polyelectrolyte multilayers.* Acta Biomater 2008. **4**: p. 827–837.
35. Spezzacatena, C., et al., *Classical synthesis of and structural studies on a biologically active heptapeptide and a nonapeptide of bovine elastin.* Eur J Org Chem, 2002. **1**: p. 95-103.
36. Tamburro, A.M., B. Bochicchio, and A. Pepe, *Dissection of Human Tropoelastin: Exon-By-Exon Chemical Synthesis and Related Conformational Studies.* Biochemistry 2003. **42**(45): p. 13347-13362.
37. Urry, D.W., *Physical Chemistry of Biological Free Energy Transduction As Demonstrated by Elastic Protein-Based Polymers.* J. Phys. Chem. B 1997. **101**(51): p. 11007–11028.
38. Bin Li and V. Daggett, *The molecular basis of the temperature- and pH-induced conformational transitions in elastin-based peptides.* Biopolymers, 2003. **68**(1): p. 121-129.

39. Urry, D.W., et al., *Temperature of polypeptide inverse temperature transition depends on mean residue hydrophobicity* J. Am. Chem. Soc., 1991. **113**: p. 4346–4348.
40. Urry, D.W., *The change in Gibbs free energy for hydrophobic association: derivation and evaluation by means of inverse temperature transitions.* Chem. Phys. Lett. , 2004. **399**: p. 177–183.
41. Meyer, D.E. and A. Chilkoti, *Quantification of the effects of chain length and concentration on the thermal behavior of elastin-like polypeptides.* Biomacromolecules, 2004. **5**: p. 846–851.
42. Cho, Y.H., et al., *Effects of hofmeister anions on the phase transition temperature of elastin-like polypeptides.* J. Phys. Chem. B., 2008. **112**: p. 13765–13771.
43. Mackay, J.A., et al., *Quantitative model of the phase behavior of recombinant pH-responsive elastin-like polypeptides.* Biomacromolecules, 2010. **11**: p. 2873–2879.
44. Callahan, D.J., et al., *Triple stimulus-responsive polypeptide nanoparticles that enhance intratumoral spatial distribution.* Nano Lett. , 2012. **12**: p. 2165–2170.
45. Bahniuk, M.S., et al., *Self-assembly/disassembly hysteresis of nanoparticles composed of marginally soluble, short elastin-like polypeptides.* Journal of Nanobiotechnology, 2018. **16**(15): p. 1-19.
46. Jiang, J., G. Oberdörster, and P. Biswas, *Characterization of size, surface charge, and agglomeration state of nanoparticle dispersions for toxicological studies.* J. Nanoparticle Res., 2009. **11**: p. 77-89.
47. Shah, R., et al., *Optimisation and stability assessment of solid lipid nanoparticles using particle size and zeta potential.* J. Phys. Sci., 2014. **25**: p. 59.
48. Elvin Blanco, H.S.M.F., *Principles of nanoparticle design for overcoming biological barriers to drug delivery.* Nature Biotechnology, 2015. **33**: p. 941-951.
49. Lundqvist, M., et al., *Nano-particle size and surface properties determine the protein corona with possible implications for biological impacts.* Proc Natl Acad Sci USA., 2008. **105**: p. 14265–70.
50. Salvi, A.S., et al., *Influence of amino acid specificities on the molecular and supramolecular organization of glycine-rich elastin-like polypeptides in water.* Biopolymers, 2011. **95**: p. 702-721.

51. Martino, M., A. Coviello, and A.M. Tamburro, *Synthesis and structural characterization of poly(LGGVG), an elastin-like polypeptide.* International Journal of Biological Macromolecules, 2000. **27**(1): p. 59-64.
52. Gaucher, G., et al., *Block copolymer micelles: preparation, characterization and application in drug delivery.* J Control Release, 2005. **109**(1-3): p. 169-188.
53. Discher, B.M., et al., *Polymersomes: tough vesicles made from diblock copolymers.* Science, 1999. **284**(5417): p. 1143-1146.
54. Bassett, D.C., F.C. Frank, and A. Keller, *Lamellae and their Organization in Melt-Crystallized Polymers [and Discussion].* Philosophical Transactions of the Royal Society of London. Series A :Physical and Engineering Sciences, 1994. **348**(1686): p. 29-43.
55. Lee, T.A.T., et al., *Thermo-Reversible Self-Assembly of Nanoparticles Derived from Elastin-MimeticPolypeptides.* Adv. Mater, 2000. **12**: p. 1105-1110.
56. Misbah, M.H., et al., *Evolution of amphiphilic elastin-like co-recombinamer morphologies from micelles to a lyotropic hydrogel.* Polymer, 2015. **81**: p. 37-44.
57. Dreher, M.R., et al., *Temperature Triggered Self-Assembly of Polypeptides into Multivalent Spherical Micelles.* J. Am. Chem. Soc., 2008. **130**: p. 687-694.
58. Janib, S.M., et al., *A quantitative recipe for engineering protein polymer nanoparticles.* Polym. chem., 2014. **5**: p. 1614-1625.
59. Dutta, N.K., et al., *A Genetically engineered protein responsive to multiple stimuli.* Angew. Chem., Int. Ed., 2011. **50**: p. 4428– 4431.
60. Weitzhandler, I., et al., *Micellar self-assembly of perfectly sequence-defined recombinant resilin-like/elastin-like block copolypeptides.* Biomacromolecules, 2017. **18**(8): p. 2419-2426.
61. Navarro, L.A., et al., *Microphase Separation of Resilin-like and Elastin-like Diblock Copolypeptides in Concentrated Solutions.* BIomacromolecules 2021. **22**: p. 3827-3838.
62. Basheer, A., et al., *Switchable Self-Assembly of Elastin- and Resilin-Based Block Copolypeptides with Converse Phase Transition Behaviors.* ACS Applied Materials & Interfaces, 2021. **13**(21): p. 24385-24400.
63. Luo, T. and K.L. Kiick, *Noncovalent Modulation of the Inverse Temperature Transition and Self-Assembly of Elastin-b-Collagen-like Peptide Bioconjugates.* J. Am. Chem. Soc. , 2015. **137**: p. 15362−15365.

64. Wang, B., et al., *Short intrinsically disordered polypeptide–oligonucleotide conjugates for programmed self-assembly of nanospheres with temperature-dependent size controllability.* Soft matter, 2021. **17**: p. 1184-1188.
65. Aluri, S., et al., *Elastin-Like Peptide Amphiphiles Form Nanofibers with Tunable Length.* Biomacromolecules, 2012. **13**: p. 2645−2654.
66. Huang, A., et al., *Predicting Protein−Polymer Block Copolymer Self-Assembly from Protein Properties.* Biomacromolecules, 2019. **20**: p. 3713−3723.
67. Qin, G., et al., *Effect of ELP Sequence and Fusion Protein Design on Concentrated Solution Self-Assembly.* Biomacromolecules, 2016. **17**: p. 928−934.
68. McDaniel, J.R., et al., *Self-assembly of thermally responsive nanoparticles of a genetically encoded peptide polymer by drug conjugation.* Angew Chem Int Ed Engl., 2013. **52**(6): p. 1683-1687.
69. Qin, G., et al., *Topological Effects on Globular Protein-ELP Fusion Block Copolymer Self-Assembly.* Adv. Funct. Mater, 2015. **25**: p. 729–738.
70. Mills, C.E., Zachary Michaud, and B.D. Olsen, *Elastin-like Polypeptide (ELP) Charge Influences Self-Assembly of ELP−mCherry Fusion Proteins.* Biomacromolecules 2018. **19**(7): p. 2517-2525.
71. Dong, X.-H., A.C. Obermeyer, and B.D. Olsen, *Three-Dimensional Ordered Antibody Arrays Through Self-Assembly of Antibody–Polymer Conjugates.* Angewandte Chemie, 2016. **56**(5): p. 1273-1277.
72. Haney, E.F., et al., *Aggregation and Its Influence on the Immunomodulatory Activity of Synthetic Innate Defense Regulator Peptides.* Cell Chemical Biology, 2017. **24**: p. 969–980.
73. Quintanilla-Sierra, L., C. García-Arévalo, and J.C. Rodriguez-Cabello, *Self-assembly in elastin-like recombinamers: a mechanism to mimic natural complexity.* Materials Today Bio, 2019. **2**: p. 100007.
74. Tantakitti, F., et al., *Energy landscapes and functions of supramolecular systems.* Nat Mater, 2016. **15**(4): p. 469-476.
75. Coenen, A.M.J., et al., *Elastic materials for tissue engineering applications: natural, synthetic, and hybrid polymers.* . Acta Biomater., 2018. **79**: p. 60-82.

76. Roberts, E.G., et al., *Fabrication and characterization of recombinant silk-elastin-like-protein (SELP) fiber.* Macromol. Biosci., 2018. **18**(12): e1800265.
77. Xia, X., et al., *Tunable Self-Assembly of Genetically Engineered Silk–Elastin-like Protein Polymers.* Biomacromolecules, 2011. **12**: p. 3844–3850.
78. Qiu, W., et al., *Complete Recombinant Silk-Elastinlike Protein-Based Tissue Scaffold.* Biomacromolecules, 2010. **11**: p. 3219–3227.
79. Isaacson, K.J., et al., *Self-assembly of thermoresponsive recombinant silk-elastinlike nanogels.* Macromol Biosci., 2018. **18**(1): p. 1700192.
80. Xia, X.-X., et al., *Hydrophobic Drug-Triggered Self-Assembly of Nanoparticles from Silk-Elastin-Like Protein Polymers for Drug Delivery.* Biomacromolecules, 2014. **15**(3): p. 908-914.
81. Lim, D.W., et al., *Rapid cross-linking of elastin-like polypeptides with (hydroxymethyl)phosphines in aqueous solution.* Biomacromolecules, 2007 **8**(5): p. 1463-1470.
82. Reichheld, S.E., et al., *Conformational transitions of the cross-linking domains of elastin during self-assembly.* J Biol Chem 2014. **289**(14): p. 10057-10068.
83. Wang, H., et al., *Covalently Adaptable Elastin-Like Protein–Hyaluronic Acid (ELP–HA) Hybrid Hydrogels with Secondary Thermoresponsive Crosslinking for Injectable Stem Cell Delivery.* Advanced functional materials 2017. **27**(28): p. 1605609.
84. Yang, Y.J., et al., *Mechanically Durable and Biologically Favorable Protein Hydrogel Based on Elastic Silklike Protein Derived from Sea Anemone.* Biomacromolecules, 2015. **16**: p. 3819-3826.
85. Camp, C.P., et al., *Non-cytotoxic Dityrosine Photocrosslinked Polymeric Materials With Targeted Elastic Moduli.* Frontiers in Chemistry, 2020. **8**(173): Article 173.
86. Li, Y. and J.A. Champion, *Photocrosslinked, Tunable Protein Vesicles for Drug Delivery Applications.* Advanced health materials 2021. **10**: p. 2001810.
87. Chen, W., et al., *Phenylboronic acid-incorporated elastin-like polypeptide nanoparticle drug delivery systems.* Polym. Chem.,, 2017. **8**: p. 2105-2114.
88. Wang, H. and S.C. Heilshorn, *Adaptable Hydrogel Networks with Reversible Linkages for Tissue Engineering.* Advanced Materials, 2015. **27**(25): p. 3717-3736.

89. Sumiyoshi, S., et al., *Development of truncated elastin-like peptide analogues with improved temperature-response and self-assembling properties.* Scientific Reports, 2022. **12**: p. 19414.
90. Schellenberger, V., et al., *A recombinant polypeptide extends the in vivo half-life of peptides and proteins in a tunable manner.* Nat Biotechnol., 2009. **27**(12): p. 1186-U155.
91. Huang, Y.S., et al., *Engineering a pharmacologically superior form of granulocyte-colony-stimulating factor by fusion with gelatin-like-protein polymer.* Eur J Pharm Biopharm, 2010. **74**(3): p. 435-41.
92. Amiram, M., et al., *Injectable protease-operated depots of glucagon-like peptide-1 provide extended and tunable glucose control.* P Natl Acad Sci USA, 2013. **110**(8): p. 2792-2797.
93. Kim, M., et al., *Artificially Engineered Protein Hydrogels Adapted from the Nucleoporin Nsp1 for Selective Biomolecular Transport.* Advanced materials, 2015. **27**(28): p. 4207-12.
94. Yang, Y.J., et al., *Nucleopore-Inspired Polymer Hydrogels for Selective Biomolecular Transport.* Biomacromolecules, 2018. **19**: p. 3905-3916.